

# Accepted Manuscript

IrO<sub>2</sub>-Ta<sub>2</sub>O<sub>5</sub>|Ti electrodes prepared by electrodeposition from different Ir:Ta ratios for the degradation of polycyclic aromatic hydrocarbons

Rosa Alhelí Herrada, Gustavo Acosta-Santoyo, Selene Sepúlveda-Guzmán, Enric Brillas, Ignasi Sirés, Erika Bustos

PII: S0013-4686(18)30084-7

DOI: [10.1016/j.electacta.2018.01.056](https://doi.org/10.1016/j.electacta.2018.01.056)

Reference: EA 31038

To appear in: *Electrochimica Acta*

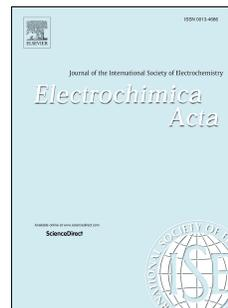
Received Date: 22 November 2017

Revised Date: 8 January 2018

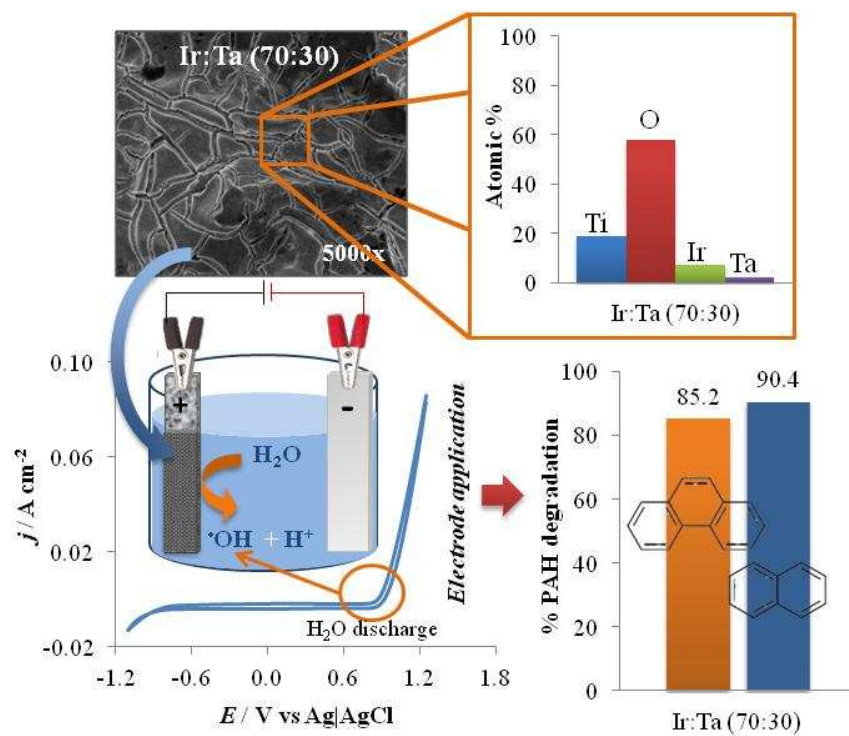
Accepted Date: 9 January 2018

Please cite this article as: Rosa.Alhelí. Herrada, G. Acosta-Santoyo, S. Sepúlveda-Guzmán, E. Brillas, I. Sirés, E. Bustos, IrO<sub>2</sub>-Ta<sub>2</sub>O<sub>5</sub>|Ti electrodes prepared by electrodeposition from different Ir:Ta ratios for the degradation of polycyclic aromatic hydrocarbons, *Electrochimica Acta* (2018), doi: 10.1016/j.electacta.2018.01.056.

This is a PDF file of an unedited manuscript that has been accepted for publication. As a service to our customers we are providing this early version of the manuscript. The manuscript will undergo copyediting, typesetting, and review of the resulting proof before it is published in its final form. Please note that during the production process errors may be discovered which could affect the content, and all legal disclaimers that apply to the journal pertain.



## GRAHICAL ABSTRACT



1 **IrO<sub>2</sub>-Ta<sub>2</sub>O<sub>5</sub>|Ti electrodes prepared by electrodeposition from different**  
2 **Ir:Ta ratios for the degradation of polycyclic aromatic hydrocarbons**

3 Rosa Alhelí Herrada<sup>a,b</sup>, Gustavo Acosta-Santoyo<sup>a</sup>, Selene Sepúlveda-Guzmán<sup>c</sup>,

4 Enric Brillas<sup>b,#</sup>, Ignasi Sirés<sup>b,\*,#</sup>, Erika Bustos<sup>a,\*\*,#</sup>

5 <sup>a</sup> *Centro de Investigación y Desarrollo Tecnológico en Electroquímica, S.C. Parque Tecnológico*  
6 *Querétaro, Sanfandila, Pedro Escobedo, 76703 Querétaro, Mexico*

7 <sup>b</sup> *Laboratori d'Electroquímica dels Materials i del Medi Ambient, Departament de Química Física,*  
8 *Facultat de Química, Universitat de Barcelona, Martí i Franquès 1-11, 08028 Barcelona, Spain*

9 <sup>c</sup> *Universidad Autónoma de Nuevo León, UANL, Facultad de Ingeniería Mecánica y Eléctrica,*  
10 *FIME, Ave. Pedro de Alba s/n, Ciudad Universitaria, C.P.66455 San Nicolás de los Garza, N.L.,*  
11 *Mexico*

12 *Paper submitted to be published in **Electrochimica Acta***

13 \* Corresponding author: Tel.: +34 934039240; fax: +34 934021231.

14 E-mail address: i.sires@ub.edu (I. Sirés)

15 \*\* Corresponding author: Tel.: +52 442 2 11 60 59; fax: +52 442 2 11 60 01.

16 E-mail address: ebustos@cideteq.mx (E. Bustos)

17 # Active ISE member

18 **Abstract**

19 This work investigates the feasibility of producing IrO<sub>2</sub>-Ta<sub>2</sub>O<sub>5</sub>/Ti electrodes by electrodeposition.  
20 Using precursor solutions with Ir:Ta molar ratios from 0:100 to 100:0, followed by thermal  
21 treatment, the goal was to find the optimal composition for enhancing the formation of hydroxyl  
22 radicals and providing long service lives. Scanning electron microscopy (SEM), coupled with  
23 energy dispersive X-ray spectroscopy (EDX), revealed that the production of homogeneous  
24 coatings with a good surface coverage and absence of agglomerates was only possible for electrodes  
25 with 70% or 100% Ir. The potential for O<sub>2</sub> evolution was similar for all the electrodes containing Ir,  
26 at about 0.90 V vs Ag|AgCl. However, the ability to produce M(<sup>•</sup>OH) clearly increased with  
27 increasing Ir in the Ir:Ta ratios (100:0 > 70:30 > 30:70 > 0:100). This observation was confirmed by  
28 the transformation of coumarin to 7-hydroxycoumarin as determined by spectroscopic and  
29 chromatographic techniques after treatment. Once manufactured and characterized, the electrodes  
30 were tested, as anodes, for the electro-oxidation of polycyclic aromatic hydrocarbons in aqueous  
31 solutions at natural pH (i.e., without pH adjustment). The anodes prepared from 70:30 and 100:0  
32 ratios produced the fastest and highest removal rates, reaching 86% and 93% for phenanthrene and  
33 naphthalene, respectively, after 120 min at 50 mA. This was accompanied by a high degree of  
34 mineralization, as the result of direct and M(<sup>•</sup>OH)-mediated oxidation, with some refractory  
35 intermediates remaining in the final solutions. The interaction between IrO<sub>2</sub> and Ta<sub>2</sub>O<sub>5</sub> oxides  
36 appeared to be important. The 100:0 anode provided high electrocatalytic effectiveness, whereas the  
37 anode with the 70:30 ratio provided improved long-term stability, as confirmed by its service life of  
38 about 93 h.

39 *Keywords:* Dimensionally stable anode; Electro-oxidation; Hydroxyl radical; PAHs; Water  
40 treatment

## 41 1. Introduction

42 Interest in electrochemical science and technology is growing worldwide, in large part because  
43 of their ability to devise new systems that ensure significant societal progress as they can lower  
44 negative environmental impacts when compared to old and well established processes [1]. The  
45 electrochemical technologies for water treatment are a clear example of this since they combine  
46 high efficiency, with low resource consumption, by using the electron as a ‘clean reagent’ [2].  
47 Within this field, the so-called electrochemical advanced oxidation processes (EAOPs) have proven  
48 most successful for the degradation of organic pollutants. In many cases it is possible to achieve the  
49 complete detoxification of water streams with their use [3,4]. This outstanding performance, when  
50 coupled with reduced energy consumption in properly designed cell configurations and the  
51 appropriate electrode materials are chosen, follows from their ability to produce reactive oxygen  
52 species (ROS), like the hydroxyl radical ( $\bullet\text{OH}$ ), in-situ and in controlled ways with the correct  
53 modulation of the electrolytic conditions.

54 Boron-doped diamond (BDD) is considered the most powerful anode for removing organic  
55 contaminants from aqueous solutions by the production of quasi-free hydroxyl radicals through the  
56 oxidation of water at a high electrode potential following the Reaction (1) [5]:



58 Despite its potential, BDD has several significant drawbacks that hamper its wider  
59 implementation on a large scale. It is expensive and very few substrate materials can be used to  
60 support stable thin films of BDD for use as anode. Additionally, the electrodes are brittle or exhibit  
61 poor electrical conductivity meaning that they are not acceptable for large scale industrial or  
62 municipal applications [6].

63 The need to reduce the cost of electrode materials has led to the synthesis of photoanodes,  
64 which allow the treatment of pollutants by an EAOP called photoelectrocatalysis [7], where  
65 artificial UV light, or natural sunlight, stimulate the production of hydroxyl radicals on the surface

66 of the photocatalysts. Alternatively, non photoactive but highly oxidizing dimensionally stable  
67 anodes suitable for O<sub>2</sub> or Cl<sub>2</sub> evolution have been manufactured by preparing mixtures of different  
68 metal oxides [8]. These anodes employ an electrocatalytic oxide film, usually based on RuO<sub>2</sub> or  
69 IrO<sub>2</sub>, deposited on a suitable metal substrate like titanium (Ti). These anodes exhibit appealing  
70 technological properties including long-term mechanical and chemical stability and high catalytic  
71 activity [2]. Aiming to increase the film stability, other oxides (e.g., TiO<sub>2</sub>, SnO<sub>2</sub>, Ta<sub>2</sub>O<sub>5</sub>) are added,  
72 thus obtaining a greater corrosion resistance and diminishing the amount of the catalytic oxide  
73 needed which, in turn, minimizes production costs [9,10]. Single- and mixed-metal oxides are then  
74 employed for the electro-oxidation (EO) of organic pollutants. EO is the paradigm of sustainability  
75 among the EAOPs, since no addition of processing chemicals is needed. Its operational simplicity,  
76 combined with high effectiveness, has led to wider implementation when compared to other  
77 EAOPs. In EO, adsorbed M(<sup>•</sup>OH) are produced by Reaction (1), with these being further  
78 transformed into a less powerful oxidant like chemisorbed “superoxide” MO [11]. Different kinds  
79 of dimensionally stable anodes have been used for the EO treatment of a large variety of organic  
80 molecules [12-21]. In the presence of Cl<sup>-</sup> ions, the complexity of EO increases significantly due to  
81 the oxidation of this anion to active chlorine according to Reaction (2), (a process exploited in the  
82 chlor-alkali industry) [6]:



84 ClO<sub>2</sub>, ClO<sup>-</sup>/HClO, ClO<sub>2</sub><sup>-</sup>, ClO<sub>3</sub><sup>-</sup> and ClO<sub>4</sub><sup>-</sup> can also be formed, depending on the operational  
85 conditions including exposure time, temperature, electrode materials and hydrodynamic conditions  
86 [22].

87 Owing to their low cost, oxide-based anodes have also found use as a counter electrode in  
88 Fenton-based EAOPs including electro-Fenton [20,23-27], electro-Fenton-like [28] and UVA or  
89 solar photoelectro-Fenton [20]. In these processes the degradation of the pollutants is mainly guided  
90 by the action of free <sup>•</sup>OH radicals generated in the bulk.

91 In spite of the reported superiority of BDD over other potential anodes, some exceptions have  
92 been reported. For example, Coria et al. [29] found a greater removal of total organic carbon (TOC)  
93 using an IrO<sub>2</sub>-based anode as compared to BDD during the treatment of naproxen by EO. This  
94 result was attributed to higher adsorption of organics on the anode surface. Results like these, when  
95 combined with improved industrial success of mixed metal oxides [30] and the higher corrosion  
96 resistance and longer service life of IrO<sub>2</sub>-based anodes as compared to RuO<sub>2</sub>-based ones [31-33],  
97 justify the interest in the optimization of the synthesis of IrO<sub>2</sub>-based dimensionally stable anodes.  
98 Specifically, those developed as a metal-oxide mixture, with Ta<sub>2</sub>O<sub>5</sub> as the stabilizer, seem the most  
99 interesting. These mixed-oxide anodes are more electrochemically stable and exhibit enhanced  
100 service life from the coating [34] than pure IrO<sub>2</sub>-based anodes.

101 In the modern world, the availability of clean water has become increasingly problematic due  
102 to both natural causes and human activity [35]. One significant problem is the presence of  
103 polycyclic aromatic hydrocarbons (PAHs), which can be produced during the incomplete  
104 combustion of organic materials including coal, oil, gas, wood, garbage, and tobacco. PAHs, due to  
105 inefficient removal processes, have been found widely in municipal wastewater and industrial  
106 effluents [36]. As a consequence of their hydrophobic nature, PAHs tend to become strongly  
107 adsorbed in sediments and aquatic organisms, as well as on the surface of particulates including  
108 micro-plastics [37], whose presence in water is also a very critical issue [38]. PAHs are included in  
109 a group of organic pollutants causing significant concern within the European Union [39], as they  
110 are suspected of being mutagens, carcinogens and endocrine disruptors [40].

111 Several authors have reported the electrochemical treatment of various PAHs with different  
112 types of mixed metal oxides [41-43]. Our teams have recently shown the feasibility of PAHs  
113 removal by EO with IrO<sub>2</sub>-based anodes synthesized using different techniques [44]. Classical  
114 synthesis routes have included thermal decomposition and the sol-gel 'Pechini' method [28].  
115 Reactive sputtering [45] and physical vapor deposition [46] are other existing alternatives. This

116 work addresses the synthesis of IrO<sub>2</sub>-Ta<sub>2</sub>O<sub>5</sub>-coated Ti-electrodes by electrodeposition using four  
117 different Ir:Ta ratios, to determine the optimal composition to stimulate the maximum concentration  
118 of hydroxyl radicals to be available for treatment. All the electrodes were characterized by scanning  
119 electron microscopy (SEM) coupled with energy dispersive X-ray spectroscopy (EDX), cyclic  
120 voltammetry (CV) and accelerated life testing. During EO testing, the production of M(<sup>•</sup>OH) was  
121 monitored using either UV/vis spectrophotometry or liquid chromatography with fluorescence  
122 detection. The oxidation power of these electrodes was verified by using them as anodes in the EO  
123 treatment of synthetic aqueous solutions containing naphthalene or phenanthrene, monitoring the  
124 concentration decay by high performance liquid chromatography (HPLC) and their mineralization  
125 from the analysis of TOC abatement.

## 126 **2. Materials and methods**

### 127 *2.1. Electrode manufacture*

128 The precursor solutions were prepared using H<sub>2</sub>IrCl<sub>6</sub> [31-34] and TaCl<sub>5</sub> [47], both purchased  
129 from Strem Chemicals ( $\geq 99.9\%$  purity). They were then dissolved in HCl [44] and isopropanol  
130 [34,44], respectively, under vigorous stirring. Four different test precursor solutions were further  
131 prepared to be used in the coating process by mixing the appropriate amount of prepared metal  
132 solutions to obtain Ir:Ta molar ratios of 100:0, 70:30, 30:70, and 0:100. Before electrodeposition,  
133 the Ti-plates (each 5.0 mm  $\times$  15.0 mm  $\times$  1.0 mm) that were to be used as substrates were pretreated  
134 by sandblasting [34,44], etching in a 40% oxalic acid solution for 20 min [31,44], and finally rinsed  
135 with deionized water and dried. Electrochemical deposition was performed at a constant current  
136 density of 14 mA cm<sup>-2</sup> for 20 min under constant stirring at 825 rpm [44]. Once the coated Ti-  
137 electrodes were prepared, the coatings were transformed into metal oxides using a 2-step thermal  
138 decomposition procedure: heating at 523 K for 10 min, followed by heating to 723 K and holding  
139 for 1 h [34,44]. Three electrodes, at each of the four coatings compositions, were prepared.

140 2.2. *Electrode characterization*

141 Microstructural analysis, to study the morphology of the deposits, was performed by SEM-  
142 EDX using a Jeol JSM6500 microscope, operating at 15 kV. Surface distribution of Ir and Ta was  
143 performed in the SEM using the Oxford Inca 300 EDX analyzer.

144 Electrochemical characterizations were made using cyclic voltammetry in a conventional three  
145 electrode glass cell. Each of the various test IrO<sub>2</sub>-Ta<sub>2</sub>O<sub>5</sub>|Ti electrodes was placed as the working  
146 electrode (0.75 cm<sup>2</sup>), with a platinum (Pt) wire (BASi) and an Ag|AgCl (3M KCl, BASi) used as  
147 counter and reference electrodes, respectively, in the cell. All experiments were performed at 298 K  
148 with 10 mL of 0.5 M H<sub>2</sub>SO<sub>4</sub> (J. T. Baker, 98%) as supporting electrolyte and employing a  
149 Bioanalytical Systems BAS-Epsilon™ potentiostat. Before the electrochemical tests, O<sub>2</sub> was purged  
150 from the test cell by bubbling ultrapure nitrogen (Praxair, grade 5.0) through the electrolyte for at  
151 least 20 min, and this gas continuously flowed over the solution during the measurement cycles. In  
152 all the cyclic voltammograms shown in this work, the active area of each coated Ti-electrode has  
153 been considered, as previously described [44]. For each of the different working electrode  
154 compositions the tests were performed in triplicate.

155 The service life of each of the various IrO<sub>2</sub>-Ta<sub>2</sub>O<sub>5</sub>|Ti coated electrodes was evaluated according  
156 to the methodology reported in NACE TM0108 [48]. A two-electrode electrochemical cell was  
157 employed, placing the coated electrodes as the working electrode (0.75 cm<sup>2</sup>) and an uncoated Ti-  
158 plate as a counter electrode (3.5 cm<sup>2</sup>). These experiments were performed at 298 K with 70 mL of 1  
159 M H<sub>2</sub>SO<sub>4</sub> as supporting electrolyte using a constant current of 3.18 A (supplied by an EZ Digital  
160 model GP-4303DU DC power supply), and with constant stirring at 825 rpm. As required in the  
161 NACE TM0108 protocol, these tests were run until an increase of 30% was observed in the inter-  
162 electrode potential difference compared to the initial value.

163 The production of hydroxyl radicals was evaluated from tests monitoring the transformation of  
164 coumarin to 7-hydroxycoumarin [49]. For this, several electrolytic tests were performed using a

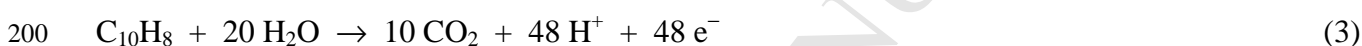
165 two-electrode electrochemical glass cell equipped with an anode, using one of each of the  
166 compositional variation IrO<sub>2</sub>-Ta<sub>2</sub>O<sub>5</sub>|Ti electrodes (0.75 cm<sup>2</sup>), and a Pt-wire as the cathode. Solutions  
167 of 10 mL of 0.3 mM coumarin (Sigma-Aldrich, 99%) in 0.5 M H<sub>2</sub>SO<sub>4</sub> were electrolyzed at room  
168 temperature and 50 mA under constant stirring. Samples were withdrawn at selected time periods to  
169 monitor changes in the concentration of coumarin. Testing by UV/vis spectroscopy, on a Shimadzu  
170 UV-1800 UV-Vis spectrophotometer within the range between 200 and 800 nm, was used during  
171 these characterizations. For the same samples, the accumulation of 7-hydroxycoumarin was  
172 assessed by HPLC using a Shimadzu LC-10ADVP chromatograph equipped with a Thermo  
173 Electron Hypersil ODS (5 μm, 150 mm × 3 mm) column coupled to a Shimadzu RF-10AXL  
174 fluorescence detector. An acetonitrile:water (60:40, v/v) mixture was used as a mobile phase to  
175 elute the samples at a flow rate of 0.5 mL min<sup>-1</sup>, with excitation and emission wavelengths of 325  
176 nm and 400 nm, respectively. A 7-hydroxycoumarin analytical standard from Sigma-Aldrich was  
177 used for quantification.

### 178 2.3. Electrochemical degradation of hydrocarbons

179 Bulk electrolyses for the performance evaluation of the manufactured electrodes to degrade  
180 PAHs, such as phenanthrene and naphthalene, were made in a two-electrode electrochemical cell,  
181 using the various IrO<sub>2</sub>-Ta<sub>2</sub>O<sub>5</sub>|Ti electrodes (0.75 cm<sup>2</sup>) and a Pt-plate as the anode and cathode.  
182 Solutions of 50 mL containing either 2 μM phenanthrene (from Acros Organics, 97%) or 2 μM  
183 naphthalene (from Alfa Aesar, 99%) in 0.05 M Na<sub>2</sub>SO<sub>4</sub> at natural pH (i.e., without pH adjustment)  
184 were treated at room temperature under a constant current of 50 mA and with constant stirring. To  
185 investigate the decay kinetics of each pollutant, samples were withdrawn at selected times for 120  
186 min and analyzed using a Waters 600 liquid chromatograph fitted with a BDS Hypersil C18 6 μm,  
187 250 mm × 4.6 mm, column at 35 °C and coupled to a Waters 996 photodiode array detector set at λ  
188 of 254 nm. These measurements were made by injecting 20 μL aliquots into the chromatograph  
189 using a 60:40 (v/v) acetonitrile/water mixture at 1.3 mL min<sup>-1</sup> as mobile phase. Peaks at 7.7 and

190 13.7 min were found for naphthalene and phenanthrene, respectively. Organic solvents and other  
 191 chemicals were of HPLC or analytical grade from Sigma-Aldrich and Panreac. All the solutions  
 192 were prepared using ultrapure water from a Millipore Milli-Q system (resistivity >18 MΩ cm).

193 To assess the mineralization ability of the anodes, the TOC content was monitored during the  
 194 treatment of 50 mL of 25 mg·L<sup>-1</sup> TOC (0.19 ) naphthalene in 0.05 M Na<sub>2</sub>SO<sub>4</sub>, at room temperature  
 195 and 50 mA under constant stirring of 825 rpm (with natural pH), using the same experimental setup  
 196 mentioned and employed above. Samples were measured on a Shimadzu VCSN TOC analyzer,  
 197 after filtration with 0.45 μm PTFE filters (Whatman) over a 360 min test cycles. The results were  
 198 obtained with ±1% accuracy. The following reaction for total mineralization of naphthalene was  
 199 assumed:



201 The mineralization current efficiency (MCE) values were estimated as follows [20]:

$$202 \% \text{MCE} = \frac{n F V \Delta(\text{TOC})_{\text{exp}}}{4.32 \times 10^7 m I t} \times 100 \quad (4)$$

203 where  $n = 48$  is the number of electrons for the mineralization,  $m = 10$  is the number of carbon  
 204 atoms of naphthalene, and all the other parameters have been defined elsewhere [20].

### 205 3. Results and discussion

#### 206 3.1. Microstructural and electrochemical characterization

207 Fig. 1A (at 2000x) and 1B (at 5000x) shows the surface morphologies of the four different  
 208 IrO<sub>2</sub>-Ta<sub>2</sub>O<sub>5</sub> coating layers found on the Ti-substrates after electrodeposition and heat cycling. In the  
 209 coatings prepared using Ir:Ta ratios of 100:0 and 70:30, it is possible to observe the cobblestone  
 210 morphology that is typical from this kind of mixed metal oxides manufactured at high temperature,  
 211 and please note its enhanced prominence in 70:30 coating. However, their surface appearance did  
 212 not exactly match a dried-mud cracked coating (i.e., mud-like islands surrounded by cracks) usually

213 observed after thermal decomposition at  $\geq 450$  °C [50]. The distribution of cracks (see red arrows)  
214 was not uniform over the entire surface as some areas were relatively flat and smooth. This may be  
215 attributed to the particular distribution of Ir and Ta on the surface during the electrodeposition step.  
216 Distributions using this method are clearly different from those resulting from a conventional  
217 painting process or by immersion of the Ti-plate into a precursor solution. As a result, the fast  
218 volatilization of solvents along with the high stress induced from anisotropic thermal expansion  
219 (different expansion coefficients of Ti and coating) seem to be substantially minimized with the  
220 electrochemical deposition treatment. This yields a more compact coating with no cracks connected  
221 over long distances, eventually reducing the possibility of coating peeling-off. In contrast, in the  
222 coatings prepared from predominately Ta ratios (30:70 and 0:100), whose microstructure when  
223 viewed at higher magnification is shown in Fig. 1B, the presence of aggregates with greater  
224 roughness can be identified (as indicated by green arrows). This suggests poor mixing of metal  
225 oxides during electrodeposition, which would likely be detrimental for further application. A poor  
226 distribution of Ta<sub>2</sub>O<sub>5</sub> will lead to poor separation between the substrate and the IrO<sub>2</sub> catalytic layer,  
227 promoting the passivation of the Ti-base metal. The presence of these kinds of agglomerates has  
228 also been reported for layers formed using non-electrochemical procedures [34].

229 Fig. 2 shows the atomic percentages of Ti, Ir, Ta and oxygen determined by EDX for the four  
230 different IrO<sub>2</sub>-Ta<sub>2</sub>O<sub>5</sub>/Ti electrodes under study. No chloride, which could have been sourced from  
231 the solutions used for the electrodeposition, was detected. The relative content of titanium and  
232 oxygen is similar for the electrodes prepared from solutions at 100:0, 70:30 and 30:70 ratios, and  
233 the proportion of Ir and Ta changes (as expected) from one to another. Importantly, the proportions  
234 are in quite good agreement with the Ir:Ta molar ratios employed in each precursor solution. The  
235 consistency of the resulting mixed metal oxide compositions suggested the absence of segregation,  
236 a very positive feature that also occurs when using sol-gel preparation methods like Pechini's [31].  
237 In the coating prepared using only the Ta-containing precursor, the amount of titanium measured

238 was higher than expected and that of Ta was too low, a result suggesting that without Ir the  
239 deposition of Ta is neither homogeneous nor quantitative, leading to a partially uncoated Ti-  
240 substrate. Therefore, this low quality electrode might well be expected to perform worse than the  
241 others.

242 Fig. 3 presents the cyclic voltammograms recorded from test employing the four IrO<sub>2</sub>-Ta<sub>2</sub>O<sub>5</sub>/Ti  
243 electrodes in 0.5 M H<sub>2</sub>SO<sub>4</sub> at room temperature and a scan rate of 50 mV s<sup>-1</sup>. The response for an  
244 uncoated Ti-substrate is not included but has been reported in earlier reports [44]. In this earlier  
245 study, no current steps were noted until a steep increase appeared in the anode potential vs Ag|AgCl  
246 at 0.05-0.10 V, which can be expected due to the low oxidation power of pure Ti-anodes. On the  
247 other hand, here it is possible to observe that for the three electrodes modified with IrO<sub>2</sub>, the O<sub>2</sub> gas  
248 evolution occurred at a potential close to 0.90 V. According to Reaction (1), adsorbed hydroxyl  
249 radicals (M(<sup>•</sup>OH)) should be generated as a first step, prior to gas evolution, and hence, their  
250 existence is investigated below. In addition, it can be seen that the increase in IrO<sub>2</sub> content in the  
251 coating, upon use of a higher initial Ir:Ta molar ratio from 30:70 to 100:0, enhances the response of  
252 the dimensionally stable anode, as deduced from the gradually greater current measured at a given  
253 potential over the oxygen evolution reaction (OER) region. Conversely, the electrochemical  
254 response of the electrode prepared with only Ta in the precursor solution (0:100 ratio) was much  
255 less significant using the same analytical sensitivity threshold. Thus, it can be concluded that Ta<sub>2</sub>O<sub>5</sub>  
256 does not perform well as an electrocatalytic oxide for hydroxyl radical formation, but, rather it  
257 serves as an interlayer to promote coating adhesion and corrosion resistance for long term use in  
258 anodic electrodes [34,44,47].

### 259 3.2. Production of hydroxyl radicals

260 The treatment of 10 mL of a 0.3 mM coumarin solution in 0.5 M H<sub>2</sub>SO<sub>4</sub> by EO with an IrO<sub>2</sub>-  
261 Ta<sub>2</sub>O<sub>5</sub>/Ti anode and a Pt cathode at 50 mA allowed us to study the formation of M(<sup>•</sup>OH) in two  
262 complementary ways. First, the decay of the coumarin content and second the generation of 7-

263 hydroxycoumarin formed upon hydroxylation of coumarin. Decay of coumarin was tracked by  
264 UV/vis spectrophotometry over 180 min test cycles for the various anode materials. As observed in  
265 Fig. 4, the anode without Ir (i.e., Ir:Ta ratio of 0:100) showed no decay of the coumarin absorbance,  
266 due to a lack of electrode catalytic response (Fig. 3). In contrast, all the anodes containing Ir showed  
267 decrease in coumarin content during the tests compared with the coumarin spectrum at time zero. A  
268 greater rate of decay was observed as the Ir content in the precursor solution increased from 30% to  
269 100%, confirming the catalytic ability of IrO<sub>2</sub>. In particular, significant decays were found using the  
270 70:30 and 100:0 ratios, which allows inferring a progressively larger production of M(<sup>•</sup>OH),  
271 although a more direct proof of hydroxyl radical generation is needed. For this, the samples  
272 collected at the same electrolysis times were simultaneously analyzed, by HPLC coupled to  
273 fluorescence detection, aiming to confirm and quantify the 7-hydroxycoumarin formed upon  
274 hydroxylation of coumarin.

275 Fig. 5 presents the time variation of the 7-hydroxycoumarin concentration under each test  
276 condition. The profiles confirm that as the the Ir:Ta molar ratio in the precursor solution increased  
277 from 0:100 to 100:0, higher production of M(<sup>•</sup>OH) was achieved. This is consistent with the  
278 inactivity of pure Ta<sub>2</sub>O<sub>5</sub> coatings as well as with the superior electrocatalytic power of layers with a  
279 high content of IrO<sub>2</sub> (> 30%). Note that, as an additional proof of the formation of M(<sup>•</sup>OH) in these  
280 types of electrodes, in a previous work we reported the electron paramagnetic resonance (EPR)  
281 analysis [44]. At this stage, the real performance of these IrO<sub>2</sub>-Ta<sub>2</sub>O<sub>5</sub>|Ti electrodes as potential  
282 anodes in typical treatment scenarios for the electro-oxidation of organic pollutants was studied.

### 283 3.3. Electro-oxidation of aqueous solutions of PAHs

284 The oxidation power of the four IrO<sub>2</sub>-Ta<sub>2</sub>O<sub>5</sub>|Ti electrodes for degrading toxic organic pollutants  
285 was tested in triplicate. Independent EO treatments of 50 mL of solutions containing ~ 2 μM of  
286 each hydrocarbon in 0.05 M Na<sub>2</sub>SO<sub>4</sub>, at natural pH and room temperature by applying 50 mA were  
287 carried out. Phenanthrene (see Fig 6A) and naphthalene (see Fig. 6B) were chosen as model PAHs,

288 since serious concerns have arisen about their presence in the environment. The decline in their  
289 concentration, as a function of electrolysis time, is shown in the two figures. Note, too, that the  
290 anode prepared without Ir (0:100 ratio) was able to remove 65%-70% phenanthrene (Fig. 6A) and  
291 79%-84% naphthalene (Fig. 6B) at 120 min, despite its poor ability to produce  $M(\bullet\text{OH})$  (Fig. 4 and  
292 5). This suggests the occurrence of direct anodic oxidation of both hydrocarbons at the  $\text{Ta}_2\text{O}_5/\text{Ti}$   
293 anodic surface. Direct oxidation of organic aromatic compounds upon adsorption on the anode  
294 surface has been suggested before, in phenol treatments for example [6]. Within the framework of  
295 PAHs oxidation, it is known that multiple bonds with angular arenes are particularly prone to  
296 electron loss. Phenanthrene is a typical substrate with such activated bonds [51] and thus, it can be  
297 gradually transformed into several intermediates. Anthracene, whose structure is similar to that of  
298 phenanthrene and naphthalene, has also been reported to become oxidized directly at the anode,  
299 yielding a radical carbocation that, in the presence of water, is not dimerized but hydrolyzed and  
300 further oxidized to anthraquinone [52].

301 As seen in Fig. 6A and 6B, all the electrode coatings containing Ir promoted a faster and greater  
302 degradation of both PAHs, in agreement with the induced formation of  $M(\bullet\text{OH})$  in the presence of  
303  $\text{IrO}_2$ . In the case of phenanthrene, the anode at the 70:30 ratio outperformed the others, reaching the  
304 limit of quantification (LOQ) of  $0.3 \mu\text{M}$  at 120 min, which accounts for  $> 86\%$  removal. For  
305 naphthalene, the anodes prepared with 100:0 and 70:30 ratios performed similarly and both reached  
306 the naphthalene LOQ, of  $0.15 \mu\text{M}$ , and greater than 93% removal during testing. Taken together,  
307 the decay of contaminants with and without Ir, one can conclude that the  $\text{IrO}_2\text{-Ta}_2\text{O}_5/\text{Ti}$  anodes  
308 degrade phenanthrene and naphthalene by combined direct and  $M(\bullet\text{OH})$ -mediated oxidation  
309 processes. None of the concentration abatements can be associated to pseudo-first-order reaction  
310 kinetics which would have been expected for reactions between the organic pollutant and a constant  
311 concentration of  $M(\bullet\text{OH})$  [20,29]. This fact further reinforces the idea of a simultaneous action of  
312 direct and indirect oxidation processes, whose contribution is time-dependent.

313 The ability of the four electrodes to completely destroy solution TOC was also assessed. Fig.  
314 7A depicts the TOC abatement over time during the EO of 50 mL of a 25 mg·L<sup>-1</sup> (0.19 mM)  
315 naphthalene solution in 0.05 M Na<sub>2</sub>SO<sub>4</sub> at natural pH by applying 50 mA. The anode with no IrO<sub>2</sub>  
316 exhibited a certain ability to transform the organic carbon to CO<sub>2</sub>, reaching 56% mineralization at  
317 360 min. The oxidation power of the anodes containing Ir was again evident as mineralization  
318 reached 74% TOC removal (i.e., final TOC content of 6.5 mg L<sup>-1</sup> TOC). At times less than 2 h, the  
319 anodes prepared with only Ir and at Ir:Ta ratio 70:30 behaved better than the 30:70 material, as  
320 expected due to their greater ability to form M(<sup>•</sup>OH). However, no substantial differences were  
321 observed between the three types of electrodes at the end of the electrolysis, This observation can  
322 be explained by the generation of highly refractory intermediates, like carboxylic acids, that cannot  
323 be easily degraded by M(<sup>•</sup>OH) [3]. The presence of this type of stable compound was confirmed by  
324 mineralization current efficiency profiles calculated from Eq. (4). As can be observed in Fig. 7B,  
325 which charts MCE vs. time, the efficiency was highest during the early stages of the treatment tests,  
326 reaching 8-10%, but it progressively decreased, as a result of the lower organic load and its higher  
327 refractory nature, ending in values as low as ~ 3%.

#### 328 3.4. Service life testing

329 From previous sections, it is clear that the presence of IrO<sub>2</sub> in the coatings is crucial to make  
330 degradation occur more rapidly, and to a greater extent. We noted that the improvement found in  
331 the performance by anodes coated with precursor solutions containing 70% and 100% Ir was  
332 minimal. A final comparison between them would be determined by coating stability for extended  
333 use. To study if any life-use differences existed between them, their service life was determined by  
334 applying the NACE TM0108 standard service life procedure (see experimental section). In these  
335 tests, a stable potential was initially observed, but a steep rise in potential was recorded once the  
336 resistance of the anode increased dramatically, causing its failure. Increasing electrical resistance  
337 can be attributed to the detachment (i.e., peeling-off) of the IrO<sub>2</sub>, Ta<sub>2</sub>O<sub>5</sub> or IrO<sub>2</sub>-Ta<sub>2</sub>O<sub>5</sub> coating from

338 the Ti-substrate [31]. In contrast to studies described above, a very remarkable superiority of the  
339 electrode prepared with a 70:30 ratio can be easily seen in Fig. 8. It performed for nearly 93 h  
340 before failure while each of the other three materials failed in less than 2 h. This electrode offers  
341 advantage from the differing performance characteristics of the two metal oxides. Its relatively high  
342 concentration of IrO<sub>2</sub> ensures significant production of M(<sup>•</sup>OH), while the moderate quantity of  
343 Ta<sub>2</sub>O<sub>5</sub> provides coating stability against corrosion. The absence of this oxide in the electrode  
344 prepared with 100% Ir causes a dramatic decay of its performance upon prolonged electrolysis.

345 Many researchers have studied the service lifetime of IrO<sub>2</sub>-Ta<sub>2</sub>O<sub>5</sub>|Ti anodes under galvanostatic  
346 conditions in 1 M H<sub>2</sub>SO<sub>4</sub> over the potential region corresponding to the OER. Huang, et al. [50]  
347 have recently prepared compositionally similar anodes by thermal treatment, reporting a service  
348 lifetime between 70 and 110 h. Results presented here agree with those in Comninellis et al. [9],  
349 who prepared IrO<sub>2</sub>-Ta<sub>2</sub>O<sub>5</sub>|Ti electrodes by thermal decomposition at 550 °C over a wide range of  
350 compositions from 10 to 100 mol.% Ir. They reported maximum electroactivity, along with the  
351 greatest electrode service life, for the electrodes containing 70% Ir.

#### 352 4. Conclusions

353 IrO<sub>2</sub>-Ta<sub>2</sub>O<sub>5</sub>|Ti electrodes have been successfully prepared by electrodeposition using precursor  
354 solutions containing four different Ir:Ta molar ratios, followed by a two step thermal treatment. The  
355 coated electrodes were then used as working electrodes in tests for the degradation of PAHs. The  
356 electrodes prepared with an Ir:Ta ratio of 70:30 were found to be superior during testing. This  
357 compositional ratio produced homogenous coatings showing good coverage and minimal  
358 segregation. They displayed the longest service life (about 93 as compared to all the other  
359 compositional electrodes with Ir content of 0%, 30%, and 100%). The ability of such an electrode to  
360 generate M(<sup>•</sup>OH) was confirmed by the gradual transformation of coumarin into 7-  
361 hydroxycoumarin during testing. Its applicability to EO treatment of organic pollutants was tested

362 by treating aqueous solutions of phenanthrene and naphthalene, at natural pH and low current.  
363 Removal of more than 86% and 93% (respectively) of these contaminants was observed after 120  
364 min. A large degree of mineralization was also attained after 360 min, although the anode was  
365 unable to degrade some highly refractory intermediates. The oxidation power of the electrodes  
366 prepared from precursor solutions with 30% and 100% Ir provided similar degradation, but their  
367 service life was found to be below 2 h. The electrode coated with only a Ta-containing precursor  
368 exhibited limited catalytic power but it did remove some of the pollutants, likely by a direct anodic  
369 oxidation of PAHs.

### 370 **Acknowledgments**

371 The authors acknowledge financial support from project CTQ2016-78616-R (AEI/FEDER,  
372 EU) and are grateful to Richard Lindeke, PhD, Professor Emeritus, University of Minnesota Duluth  
373 and U.S. Peace Corps Volunteer at the CIATEC (Leon, Mexico), for his English revision to this  
374 manuscript. Financial support from the Consejo Nacional de Ciencia y Tecnología de los Estados  
375 Unidos Mexicanos (CONACyT) to carry out the work and in the form of a PhD fellowship to R.A.  
376 Herrada is also acknowledged. We are also grateful to María de Montserrat Chávez Espinoza,  
377 Daniela Ramírez Padilla, Maribel Romero García and Edgar Salvador Fuentes Encinas for their  
378 collaboration with laboratory procedures.

### 379 **References**

- 380 [1] S. Bebelis, K. Bouzek, A. Cornell, M.G.S. Ferreira, G.H. Kelsall, F. Lapicque, C. Ponce de  
381 León, M.A. Rodrigo, F.C. Walsh, Highlights during the development of electrochemical  
382 engineering, *Chem. Eng. Res. Design* 91 (2013) 1998-2020.
- 383 [2] Y. Feng, L. Yang, J. Liu, B.E. Logan, Electrochemical technologies for wastewater treatment  
384 and resource reclamation, *Environ. Sci.: Water Res.* 2 (2016) 800-831.

- 385 [3] I. Sirés, E. Brillas, M.A. Oturan, M.A. Rodrigo, M. Panizza, Electrochemical advanced  
386 oxidation processes: today and tomorrow. A review, *Environ. Sci. Pollut. Res.* 21 (2014)  
387 8336-8367.
- 388 [4] C.A. Martínez-Huitle, M.A. Rodrigo, I. Sirés, O. Scialdone, Single and coupled  
389 electrochemical processes and reactors for the abatement of organic water pollutants: A  
390 critical review, *Chem. Rev.* 115 (2015) 13362-13407.
- 391 [5] A. Kapalka, G. Fóti, C. Comninellis, The importance of electrode material in environmental  
392 electrochemistry. Formation and reactivity of free hydroxyl radicals on boron-doped diamond  
393 electrodes, *Electrochim. Acta* 54 (2009) 2018-2023.
- 394 [6] M. Panizza, G. Cerisola, Direct and mediated anodic oxidation of organic pollutants, *Chem.*  
395 *Rev.* 109 (2009) 6541-6569.
- 396 [7] Y. Zhang, X. Xiong, Y. Han, X. Zhang, F. Shen, S. Deng, H. Xiao, X. Yang, G. Yang, H.  
397 Peng, Photoelectrocatalytic degradation of recalcitrant organic pollutants using TiO<sub>2</sub> film  
398 electrodes: An overview, *Chemosphere* 88 (2012) 145-154.
- 399 [8] W. Wu, Z.-H. Huang, T.-T. Lim, Recent development of mixed metal oxide anodes for  
400 electrochemical oxidation of organic pollutants in water, *Appl. Catal. A: Gen.* 480 (2014) 58-  
401 78.
- 402 [9] C. Comninellis, G.P. Vercesi, Characterization of DSA<sup>®</sup>-type oxygen evolving electrodes:  
403 Choice of a coating, *J. Appl. Electrochem.* 21 (1991) 335-345.
- 404 [10] D. Rosestolato, S. Neodo, S. Ferro, G. Battaglin, V. Rigato, A. De Battisti, A comparison  
405 between structural and electrochemical properties of iridium oxide-based electrocatalysts  
406 prepared by sol-gel and reactive sputtering deposition, *J. Electrochem. Soc.* 161 (2014) E151-  
407 E158.

- 408 [11] G. Fóti, D. Gandini, C. Cominellis, A. Perret, W. Haenni, Oxidation of organics by  
409 intermediates of water discharge on IrO<sub>2</sub> and synthetic diamond anodes, *Electrochem. Solid*  
410 *State Lett.* 2 (1999) 228-230.
- 411 [12] S. Aquino Neto, A.R. de Andrade, Electrooxidation of glyphosate herbicide at different DSA<sup>®</sup>  
412 compositions: pH, concentration and supporting electrolyte effect, *Electrochim. Acta* 54  
413 (2009) 2039-2045.
- 414 [13] O. Scialdone, S. Randazzo, A. Galia, G. Filardo, Electrochemical oxidation of organics at  
415 metal oxide electrodes: The incineration of oxalic acid at IrO<sub>2</sub>-Ta<sub>2</sub>O<sub>5</sub> (DSA-O<sub>2</sub>) anode,  
416 *Electrochim. Acta* 54 (2009) 1210-1217.
- 417 [14] O. Scialdone, A. Galia, S. Randazzo, Oxidation of carboxylic acids in water at IrO<sub>2</sub>-Ta<sub>2</sub>O<sub>5</sub>  
418 and boron doped diamond anodes, *Chem. Eng. J.* 174 (2011) 266-274.
- 419 [15] M. Pérez-Corona, A. Corona, E.D. Beltrán, J. Cárdenas, E. Bustos, Evaluation of IrO<sub>2</sub>-  
420 Ta<sub>2</sub>O<sub>5</sub>|Ti electrodes employed during the electroremediation of hydrocarbon-contaminated  
421 soil, *Sustain. Environ. Res.* 23 (2013) 279-284.
- 422 [16] B. Borbón, M.T. Oropeza-Guzman, E. Brillas, I. Sirés, Sequential electrochemical treatment  
423 of dairy wastewater using aluminum and DSA-type anodes, *Environ. Sci. Pollut. Res.* 21  
424 (2014) 8573-8584.
- 425 [17] E. Mousset, N. Oturan, E.D. van Hullebusch, G. Guibaud, G. Esposito, M.A. Oturan,  
426 Treatment of synthetic soil washing solutions containing phenanthrene and cyclodextrin by  
427 electro-oxidation. Influence of anode materials on toxicity removal and biodegradability  
428 enhancement, *Appl. Catal. B: Environ.* 160-161 (2014) 666-675.
- 429 [18] A. Galia, S. Lanzalaco, M.A. Sabatino, C. Dispenza, O. Scialdone, I. Sirés, Crosslinking of  
430 poly(vinylpyrrolidone) activated by electrogenerated hydroxyl radicals: A first step towards a  
431 simple and cheap synthetic route of nanogel vectors, *Electrochem. Commun.* 62 (2016) 64-68.

- 432 [19] M.J.R. Santos, M.C. Medeiros, T.M.B.F. Oliveira, C.C.O. Morais, S.E. Mazzetto, C.A.  
433 Martínez-Huitle, S.S.L. Castro, Electrooxidation of cardanol on mixed metal oxide (RuO<sub>2</sub>-  
434 TiO<sub>2</sub> and IrO<sub>2</sub>-RuO<sub>2</sub>-TiO<sub>2</sub>) coated titanium anodes: insights into recalcitrant phenolic  
435 compounds, *Electrochim. Acta* 212 (2016) 95-101.
- 436 [20] J.R. Steter, E. Brillas, I. Sirés, On the selection of the anode material for the electrochemical  
437 removal of methylparaben from different aqueous media, *Electrochim. Acta* 222 (2016) 1464-  
438 1474.
- 439 [21] D.T. Araújo, M.A. Gomes, R.S. Silva, C.C. de Almeida, C.A. Martínez-Huitle, K.I.B.  
440 Eguiluz, G.R. Salazar-Banda, Ternary dimensionally stable anodes composed of RuO<sub>2</sub> and  
441 IrO<sub>2</sub> with CeO<sub>2</sub>, SnO<sub>2</sub>, or Sb<sub>2</sub>O<sub>3</sub> for efficient naphthalene and benzene electrochemical  
442 removal, *J. Appl. Electrochem.* 47 (2017) 547-561.
- 443 [22] S. Neodo, D. Rosestolato, S. Ferro, A. De Battisti, On the electrolysis of dilute chloride  
444 solutions: Influence of the electrode material on Faradaic efficiency for active chlorine,  
445 chlorate and perchlorate, *Electrochim. Acta* 80 (2012) 282-291.
- 446 [23] O. Scialdone, E. Corrado, A. Galia, I. Sirés, Electrochemical processes in macro and  
447 microfluidic cells for the abatement of chloracetic acid from water, *Electrochim. Acta* 132  
448 (2014) 15-24.
- 449 [24] F. Sopaj, N. Oturan, J. Pinson, F. Podvorica, M.A. Oturan, Effect of the anode materials on  
450 the efficiency of the electro-Fenton process for the mineralization of the antibiotic  
451 sulfamethazine, *Appl. Catal. B: Environ.* 199 (2016) 331-341.
- 452 [25] S. Ellouze, S. Kessemtni, D. Clematis, G. Cerisola, M. Panizza, S.C. Elaoud, Application of  
453 Doehlert design to the electro-Fenton treatment of Bismarck Brown Y, *J. Electroanal. Chem.*  
454 799 (2017) 34-39.

- 455 [26] S. Lanzalaco, I. Sirés, M.A. Sabatino, C. Dispenza, O. Scialdone, A. Galia, Synthesis of  
456 polymer nanogels by electro-Fenton process: investigation of the effect of main operation  
457 parameters, *Electrochim. Acta* 246 (2017) 812-822.
- 458 [27] Y.-U. Shin, H.-Y. Yoo, S. Kim, K.-M. Chung, Y.-G. Park, K.-H. Hwang, S.W. Hong, H.  
459 Park, K. Cho, J. Lee, Sequential combination of electro-Fenton and electrochemical  
460 chlorination processes for the treatment of anaerobically-digested food wastewater, *Environ.*  
461 *Sci. Technol.* 51 (2017) 10700-10710.
- 462 [28] Z.G. Aguilar, E. Brillas, M. Salazar, J.L. Nava, I. Sirés, Evidence of Fenton-like reaction with  
463 active chlorine during the electrocatalytic oxidation of Acid Yellow 36 azo dye with Ir-Sn-Sb  
464 oxide anode in the presence of iron ion, *Appl. Catal. B: Environ.* 206 (2017) 44-52.
- 465 [29] G. Coria, I. Sirés, E. Brillas, J.L. Nava, Influence of the anode material on the degradation of  
466 naproxen by Fenton-based electrochemical processes, *Chem. Eng. J.* 304 (2016) 817-825.
- 467 [30] S. Trasatti, Electrocatalysis: understanding the success of DSA<sup>®</sup>, *Electrochim. Acta* 45 (2000)  
468 2377-2385.
- 469 [31] L. Xu, Y. Xin, J. Wang, A comparative study on IrO<sub>2</sub>-Ta<sub>2</sub>O<sub>5</sub> coated titanium electrodes  
470 prepared with different methods, *Electrochim. Acta* 54 (2009) 1820-1825.
- 471 [32] X. Qin, F. Gao, G. Chen, Effects of the geometry and operating temperature on the stability of  
472 Ti/IrO<sub>2</sub>-SnO<sub>2</sub>-Sb<sub>2</sub>O<sub>5</sub> electrodes for O<sub>2</sub> evolution, *J. Appl. Electrochem.* 40 (2010) 1797-1805.
- 473 [33] S. Ferro, D. Rosestolato, C.A. Martínez-Huitle, A. De Battisti, On the oxygen evolution  
474 reaction at IrO<sub>2</sub>-SnO<sub>2</sub> mixed-oxide electrodes, *Electrochim. Acta* 146 (2014) 257-261.
- 475 [34] J.-Y. Lee, An investigation on the electrochemical characteristics of Ta<sub>2</sub>O<sub>5</sub>-IrO<sub>2</sub> anodes for  
476 the application of electrolysis process, *Mater. Sci. Appl.* 2 (2011) 237-243.
- 477 [35] E. Lichtfouse, J. Schwarzbauer, D. Robert (Eds.), *Environmental chemistry for a sustainable*  
478 *world – Vol. 2: Remediation of air and water pollution*, Springer, The Netherlands, 2012.

- 479 [36] F. Fatone, S. Di Fabio, D. Bolzonella, F. Cecchi, Fate of aromatic hydrocarbons in Italian  
480 municipal wastewater systems: an overview of wastewater treatment using conventional  
481 activated-sludge processes (CASP) and membrane bioreactors (MBRs), *Water Res.* 45 (2011)  
482 93-104.
- 483 [37] W. Wang, J. Wang, Different partition of polycyclic aromatic hydrocarbon on environmental  
484 particulates in wastewater: Microplastics in comparison to natural sediment, *Ecotoxicol.*  
485 *Environ. Safety* 147 (2018) 648-655.
- 486 [38] O.M. Lönnstedt, P. Eklöv, Environmentally relevant concentrations of microplastic particles  
487 influence larval fish ecology, *Science* 352 (2016) 1213-1216.
- 488 [39] Directive 2000/60/EC of the European Parliament and of the Council establishing a  
489 framework for Community action in the field of water policy official J. L 327, 22 December  
490 2000, pp. 0001–0073 ([www.europa.eu.int](http://www.europa.eu.int)).
- 491 [40] D. Han, M.J. Currell, Persistent organic pollutants in China's surface water systems, *Sci. Total*  
492 *Environ.* 580 (2017) 602-625.
- 493 [41] J. Muff, E.G. Sjøgaard, Electrochemical degradation of PAH compounds in process water: a  
494 kinetic study on model solutions and a proof of concept study on runoff water from harbour  
495 sediment purification, *Water Sci. Technol.* 61 (2010) 2043-2051.
- 496 [42] A. Yaqub, M.H. Isa, H. Ajab, Electrochemical degradation of polycyclic aromatic  
497 hydrocarbons in synthetic solution and produced water using a Ti/SnO<sub>2</sub>-Sb<sub>2</sub>O<sub>5</sub>-RuO<sub>2</sub> anode, *J.*  
498 *Environ. Eng.* 141 (2015) 1-8.
- 499 [43] E. Pepprah, M.V. Khire, Electroremediation of naphthalene in aqueous solution using  
500 alternating and direct currents, *J. Environ. Eng.* 134 (2008) 32-41.
- 501 [44] R.A. Herrada, A. Medel, F. Manríquez, I. Sirés, E. Bustos, Preparation of IrO<sub>2</sub>-Ta<sub>2</sub>O<sub>5</sub>/Ti  
502 electrodes by immersion, painting and electrophoretic deposition for the electrochemical  
503 removal of hydrocarbons from water, *J. Hazard. Mater.* 319 (2016) 102-110.

- 504 [45] D. Rosestolato, S. Neodo, S. Ferro, G. Battaglin, V. Rigato, A. De Battisti, A comparison  
505 between structural and electrochemical properties of iridium oxide-based electrocatalysts  
506 prepared by sol-gel and reactive sputtering deposition, *J. Electrochem. Soc.* 161 (2014) E151-  
507 E158.
- 508 [46] G. Battaglin, D. Rosestolato, S. Ferro, A. De Battisti, Characterization of IrO<sub>2</sub>-SnO<sub>2</sub> films  
509 prepared by physical vapor deposition at ambient temperature, *Electrocatalysis* 4 (2013) 358-  
510 366.
- 511 [47] S. Fierro, A. Kapałka, C. Comninellis, Electrochemical comparison between IrO<sub>2</sub> prepared by  
512 thermal treatment of iridium metal and IrO<sub>2</sub> prepared by thermal decomposition of H<sub>2</sub>IrCl<sub>6</sub>  
513 solution, *Electrochem. Commun.* 12 (2010) 172-174.
- 514 [48] NACE International, Standard test method TM0108 Testing of Catalyzed Titanium Anodes  
515 for Use in Soils or Natural Waters, 2012.
- 516 [49] T. Maezono, M. Tokumura, M. Sekine, Y. Kawase, Hydroxyl radical concentration profile in  
517 photo-Fenton oxidation process: Generation and consumption of hydroxyl radicals during the  
518 discoloration of azo-dye Orange II, *Chemosphere* 82 (2011) 1422-1430.
- 519 [50] C.A. Huang, S.W. Yang, C.Z. Chen, F.-Y. Hsu, Electrochemical behavior of IrO<sub>2</sub>-Ta<sub>2</sub>O<sub>5</sub>/Ti  
520 anodes prepared with different surface pretreatments of Ti substrate, *Surf. Coat. Technol.* 320  
521 (2017) 270-278.
- 522 [51] M.R. Heinrich, A. Gansäuer (Eds.), *Radicals in Synthesis III*, Topics in Current Chemistry,  
523 Book 320, Springer-Verlag, Heidelberg, 2012.
- 524 [52] C.A. Paddon, C.E. Banks, I.G. Davies, R.G. Compton, Oxidation of anthracene on platinum  
525 macro- and micro-electrodes: Sonoelectrochemical, cryoelectrochemical and  
526 sonocryoelectrochemical studies, *Ultrason. Sonochem.* 13 (2006) 126-132.
- 527

528 **Figure captions**

529 **Figure 1.** Scanning electron micrographs of the surfaces of the IrO<sub>2</sub>-Ta<sub>2</sub>O<sub>5</sub>/Ti electrodes  
530 manufactured by electrodeposition, using four different Ir:Ta molar ratios, followed by thermal  
531 decomposition. Magnification: (A) 2000x and (B) 5000x.

532 **Figure 2.** Atomic percentages of Ti, Ir, Ta and oxygen analyzed by EDX for the four IrO<sub>2</sub>-Ta<sub>2</sub>O<sub>5</sub>/Ti  
533 electrodes manufactured with different Ir:Ta molar ratios as seen on the x axis.

534 **Figure 3.** Cyclic voltammograms recorded using each of the four IrO<sub>2</sub>-Ta<sub>2</sub>O<sub>5</sub>/Ti materials (0.75 cm<sup>2</sup>  
535 of exposed surface area), with different Ir:Ta molar ratios, as the working electrode in 0.5 M H<sub>2</sub>SO<sub>4</sub>  
536 at room temperature. Counter electrode: Pt wire. Reference electrode: Ag|AgCl (3 M KCl). Scan  
537 rate: 50 mV s<sup>-1</sup>.

538 **Figure 4.** UV/vis spectra of 10 mL of a 0.3 mM coumarin solution in 0.5 M H<sub>2</sub>SO<sub>4</sub>, electrolyzed for  
539 180 min at 50 mA and room temperature under constant stirring. Each single IrO<sub>2</sub>-Ta<sub>2</sub>O<sub>5</sub>/Ti  
540 electrode (0.75 cm<sup>2</sup>) at a given Ir:Ta molar ratio and a Pt wire were employed as the anode and  
541 cathode, respectively. The spectrum of coumarin at time zero is also shown for reference.

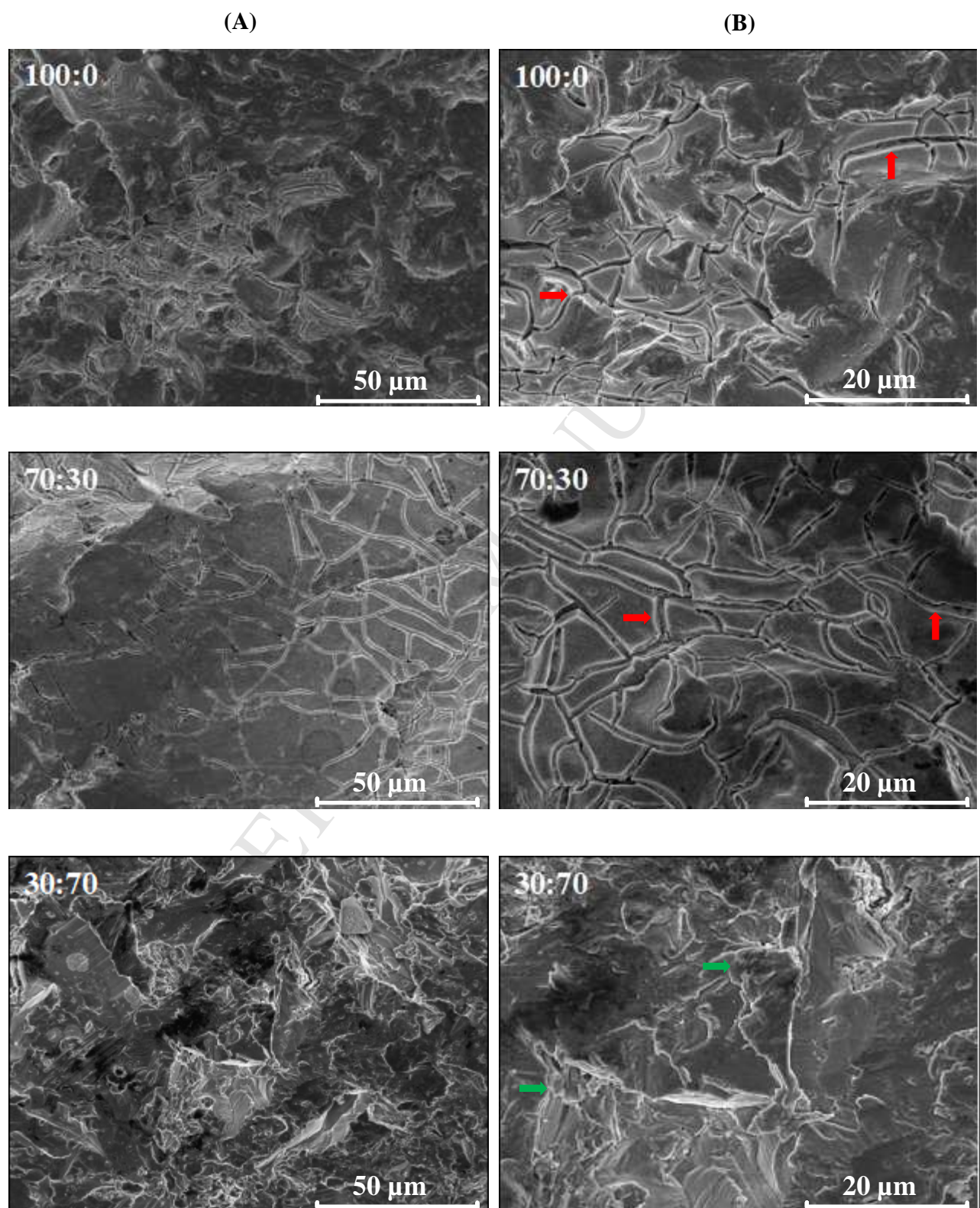
542 **Figure 5.** 7-Hydroxycoumarin concentration accumulated over time during the experiments  
543 described in Fig. 4. Data were obtained from an HPLC instrument coupled to a fluorescence  
544 detector.

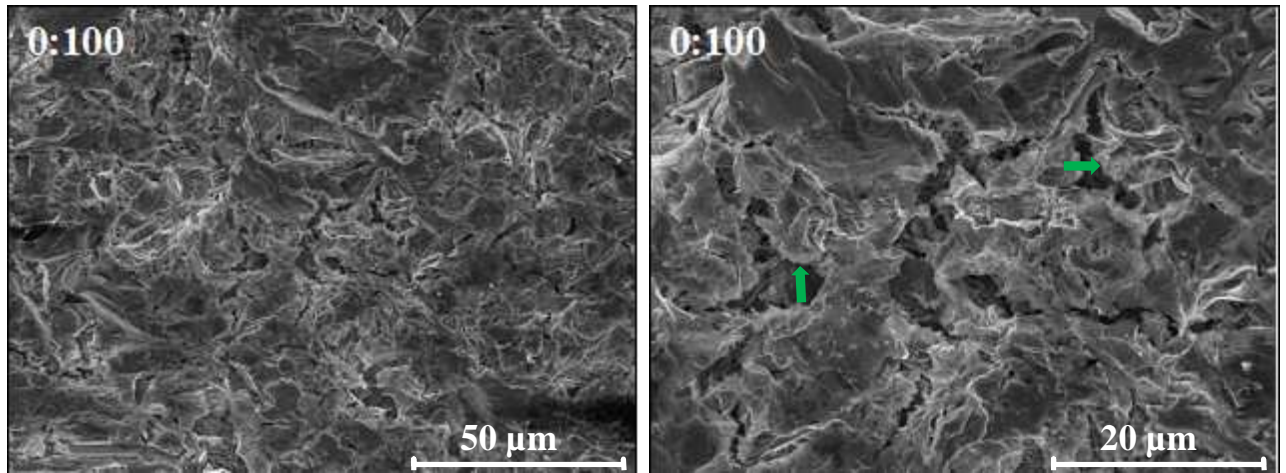
545 **Figure 6.** (A) Decay of phenanthrene concentration with electrolysis time during the electro-  
546 oxidation of 50 mL of solutions containing ~ 2 μM of the hydrocarbon in 0.05 M Na<sub>2</sub>SO<sub>4</sub> at natural  
547 pH and room temperature by applying 50 mA. Each IrO<sub>2</sub>-Ta<sub>2</sub>O<sub>5</sub>/Ti electrode (0.75 cm<sup>2</sup>) at given  
548 Ir:Ta molar ratios and a Pt plate were employed as the anode and cathode, respectively. (B) Decay  
549 of naphthalene during analogous treatments. The horizontal dashed lines represent the limit of  
550 quantification for both PAHs under the selected analytical conditions.

551 **Figure 7.** (A) TOC abatement vs time during the electro-oxidation of 50 mL of a 25 mg·L<sup>-1</sup> (0.19  
552 mM) naphthalene solution in 0.05 M Na<sub>2</sub>SO<sub>4</sub> at natural pH and room temperature by applying 50  
553 mA. Each single IrO<sub>2</sub>-Ta<sub>2</sub>O<sub>5</sub>/Ti electrode (0.75 cm<sup>2</sup>) at a given Ir:Ta molar ratio and a Pt plate were  
554 employed as the anode and cathode, respectively. (B) Mineralization current efficiency calculated  
555 from Eq. (4) for the above trials.

556 **Figure 8.** Service life of each manufactured electrode, at a given Ir:Ta molar ratio, determined  
557 according to NACE TM0108 standard procedure.

Figure 1





ACCEPTED MANUSCRIPT

Figure 2

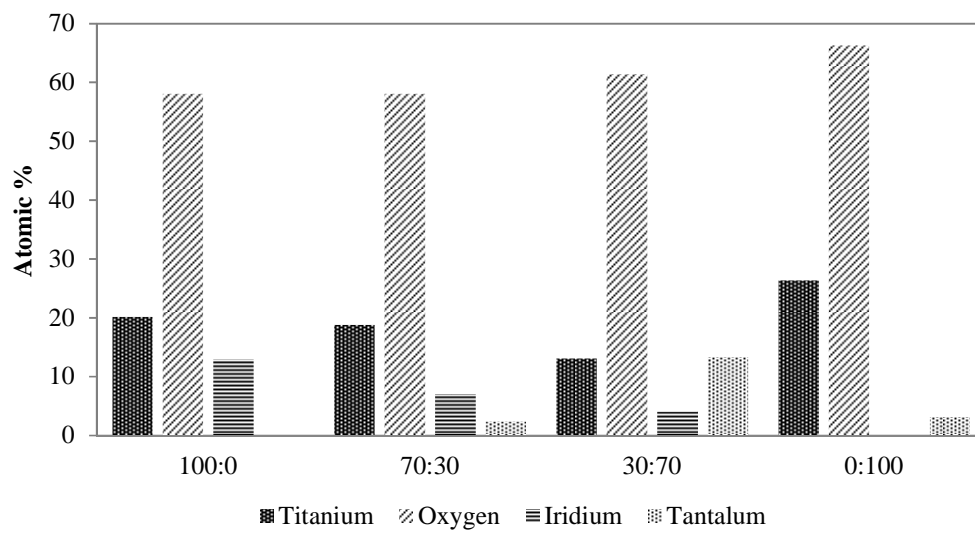
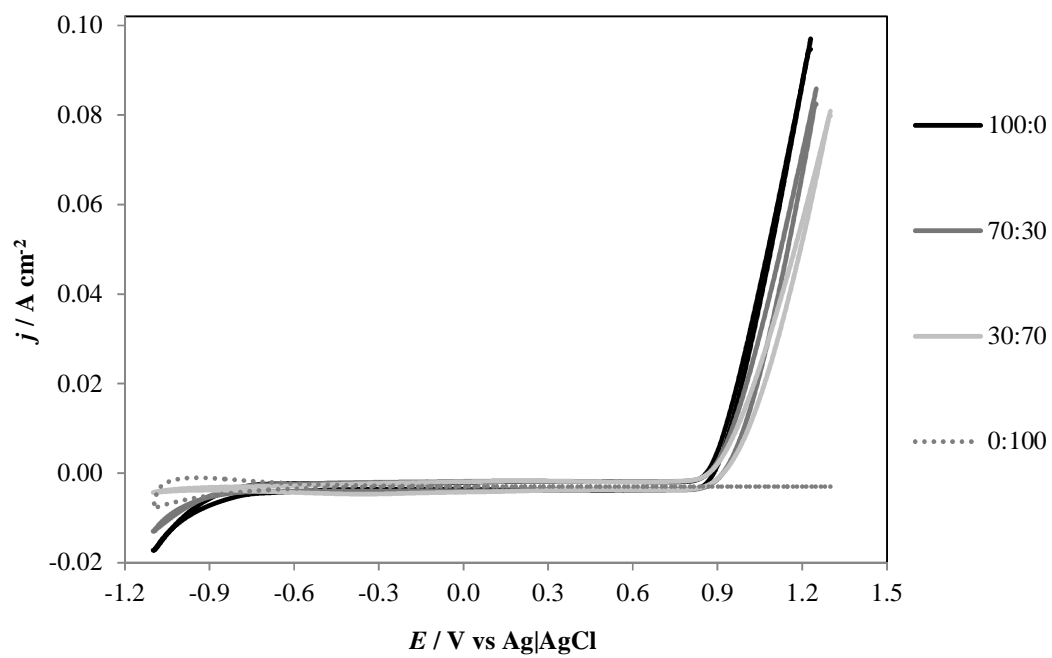


Figure 3



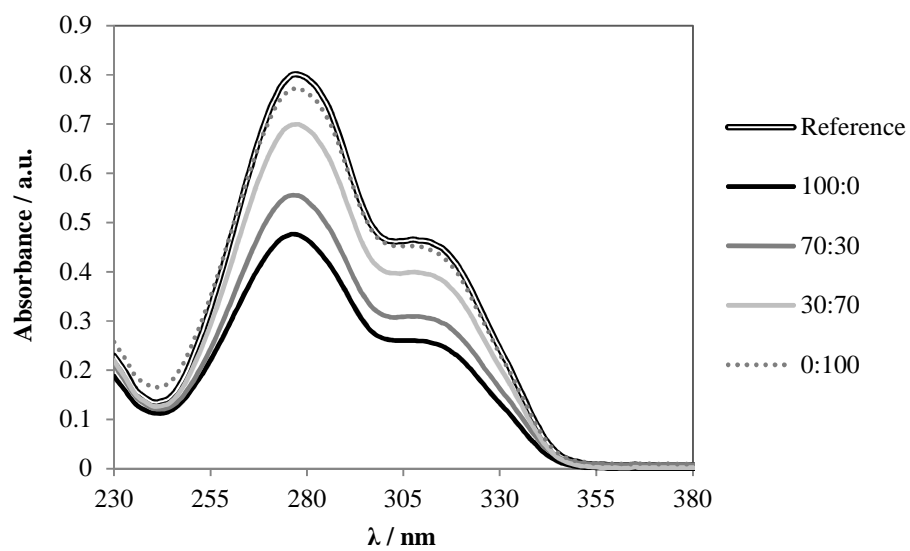
**Figure 4**

Figure 5

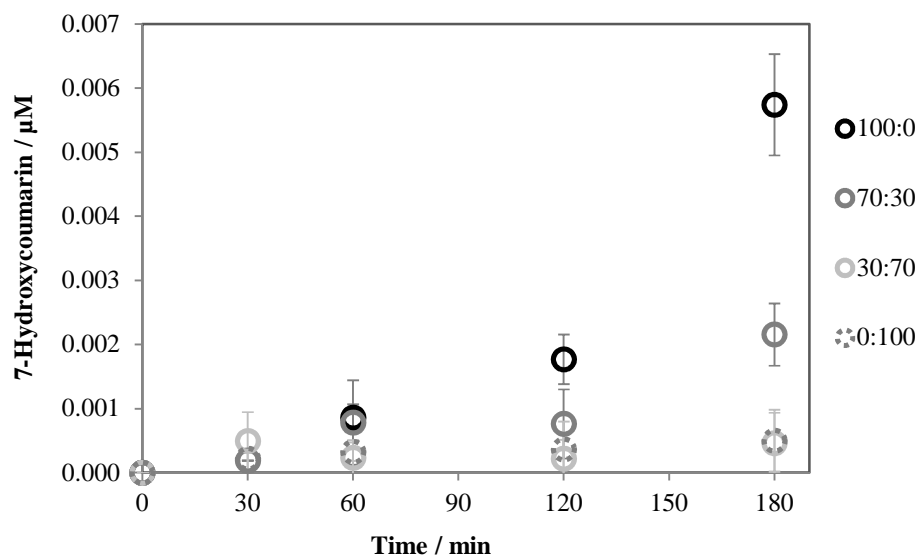
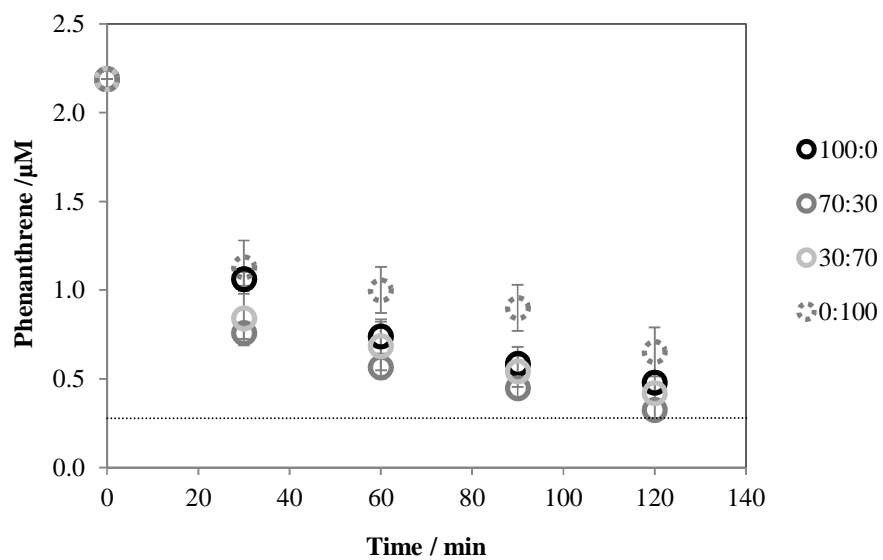


Figure 6

(A)



(B)

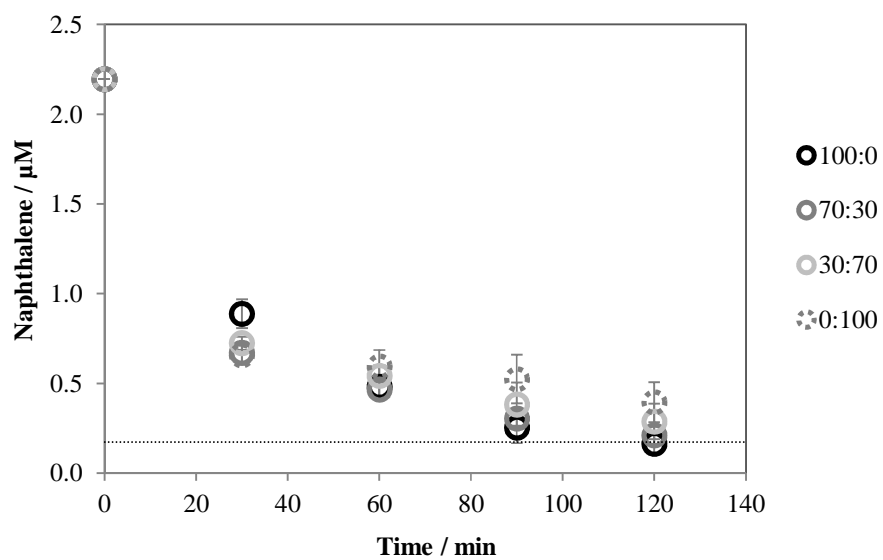
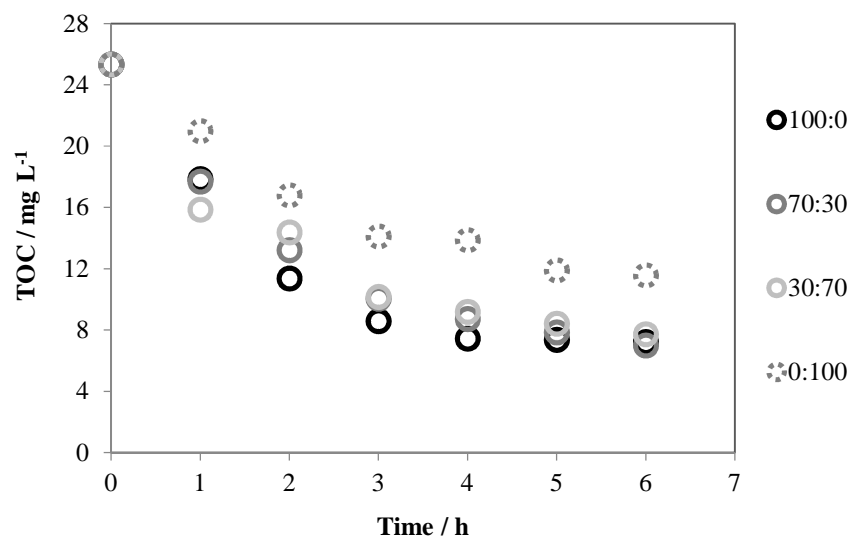
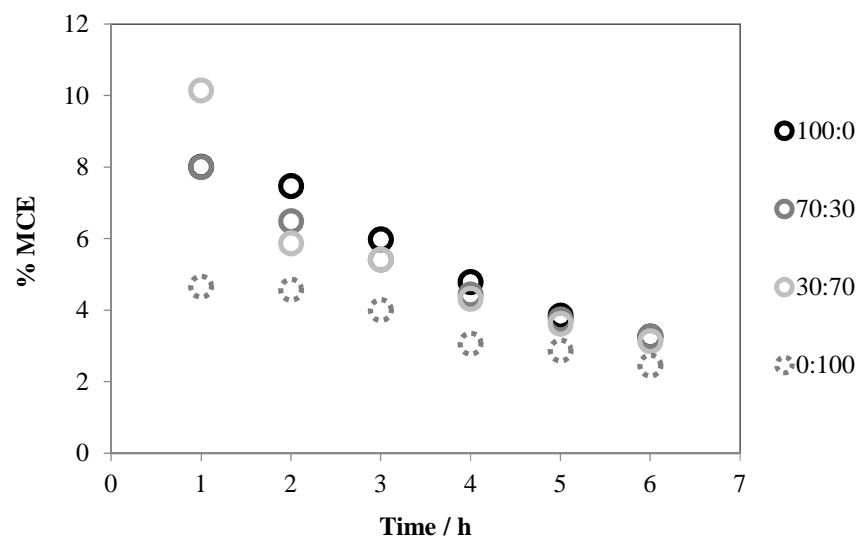


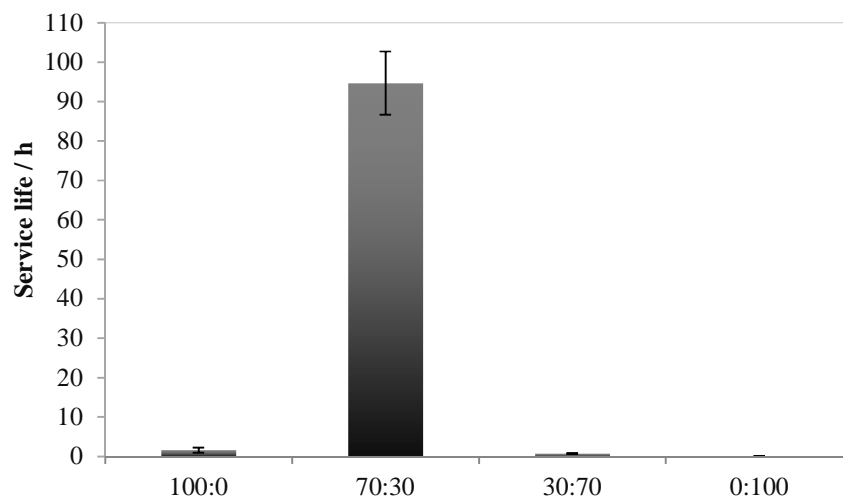
Figure 7

(A)



(B)



**Figure 8**

## Highlights

- High quality coatings by electrodeposition followed by thermal treatment: 70% or 100% Ir
- Production of  $M(^{\bullet}OH)$  clearly increased in the order (Ir:Ta): 0:100 < 30:70 < 70:30 < 100:0
- Electro-oxidation of PAHs using  $IrO_2-Ta_2O_5|Ti$  anodes: direct +  $M(^{\bullet}OH)$ -mediated oxidation
- Up to 86% and 93% removal of phenanthrene and naphthalene, along with 74% TOC abatement
- $IrO_2-Ta_2O_5|Ti$  electrode with Ir:Ta 70:30 showed highest electrocatalytic power and service life